Efficiency Mode Characterization of an Electron Cyclotron Resonance Magnetic Nozzle Thruster Operating on Nitrogen

IEPC-2025-524

Presented at the 39th International Electric Propulsion Conference, Imperial College London, London, United Kingdom
14-19 September 2025

John Riley K. O'Toole* and Ari J. Eckhaus †
University of Michigan, Ann Arbor, Michigan, 48105, USA

Benjamin A. Jorns‡
University of Michigan, Ann Arbor, Michigan, 48105, USA

The performance and efficiency modes of an electron cyclotron resonance (ECR) magnetic nozzle thruster operating on nitrogen are experimentally characterized. A sub-kW class ECR thruster is tested with a fixed nitrogen flow rate of 8 SCCM at operating powers between 20 and 50 W. Global performance is determined by thrust stand measurements, while an efficiency mode breakdown is completed with a far-field probe suite that consists of a E×B probe, a Langmuir Probe, a retarding potential analyzer, and a Faraday probe. It is found that specific impulse peaked near 400 s at 50 W of input power, and total efficiency did not exceed 2%. Mass utilization, in turn, is shown to be the primary detractor to overall thruster performance. This low utilization is discussed in the context of a simplified 1D model and compared to the nominal performance of the same thruster operating on xenon. This model is leveraged to inform recommendations for improvements in thruster operation on nitrogen.

I. Introduction

There is a growing interest in operating electric propulsion (EP) systems that can operate on non-noble gas propellants, particularly as it relates to air-breathing and multimode architectures.[1–3] However, these missions require the use of light-weight molecular propellants that are both difficult to ionize, thus lowering performance, and pose potential lifetime risks to key aspects of mature EP devices. Most notably, for commonly flown devices like Hall-effect thrusters (HETs) and gridded ion thrusters, the electron source, the cathode, is highly susceptible to poisoning from these types of propellants.

Electron Cyclotron Resonance (ECR) thrusters, a type of wave-based plasma thruster, have the potential to overcome at least one key limitation for existing EP devices operating on unconventional fuels. This stems from the fact that ECR devices employ a largely electrodeless, non-thermionic scheme to energize their propellant. This avoids the conventional issues with poisoning attributed to Hall and gridded ion thrusters. At the same time, ECR thrusters may also offer a solution to the problem of low ionization of lightweight molecular propellants as well. Indeed, there is indirect evidence to suggest that electron temperatures in ECR devices may exceed 70 eV.[4] Such high temperatures could greatly improve ionization efficiency on molecular propellants when compared to HETs, which, at the same power levels, typically produce lower temperature electrons[5].

With that said, to the best of our knowledge, ECR thrusters have only been characterized to date extensively with one molecular propellant: water.[6,7] While these studies did demonstrate the ECR architecture

*PhD. Pre-Candidate, Department of Aerospace Engineering, otoolejr@umich.edu.
†PhD. Candidate, Department of Aerospace Engineering, aeckhaus@umich.edu.
‡Associate Professor, Department of Aerospace Engineering, bjorns@umich.edu.

was compatible with water at moderate power levels (< 50 W), the total performance suffered when compared to operation on more conventional xenon propellant. Total efficiency was below 2%, and specific impulses peaked at 750s. Additional detailed work performed by Sheppard and Little revealed that low mass utilization (low ionization efficiency) was indeed the cause of overall lower efficiencies and specific impulses in their ECR thruster operating on water.[6] This suggests that at least for this lightweight molecular propellant and power level, ionization remains an outstanding challenge.

Despite these initial findings with water, there is the possibility that other molecular propellants may still have improved performance. Nitrogen, for example, is common to most next-generation propellants of interest (air and multimode) and is less complex than water, with a higher ionization cross-section. Given the advantages of nitrogen and the potential benefits of ECR for working with this gas, there is a need for an initial detailed experimental and theoretical characterization of the performance of these devices on this propellant.

To this end, the goal of this work is to evaluate the performance and constituent efficiency modes of a 30 W class ECR magnetic nozzle thruster operating on nitrogen. This paper is organized in the following way. In Section II, we discuss ECR and magnetic nozzle theory and operation with a breakdown of the efficiency modes. Section III is our experimental setup, and Section IV is a discussion of probe usage and analysis. Section V is the results from our study, with discussion in Section VI, followed by Section VII, which contains concluding remarks.

II. Theory of Operation for ECR Magnetic Nozzle Thrusters

A. Overview of thruster

ECR plasma sources have been utilized for a wide array of applications since the early 1960's. These include using ECR sources to study plasma waves, controlled fusion, semiconductor etching, and as it pertains to this study, spacecraft propulsion.[8] Figure 1 shows a basic diagram for an ECR thruster.

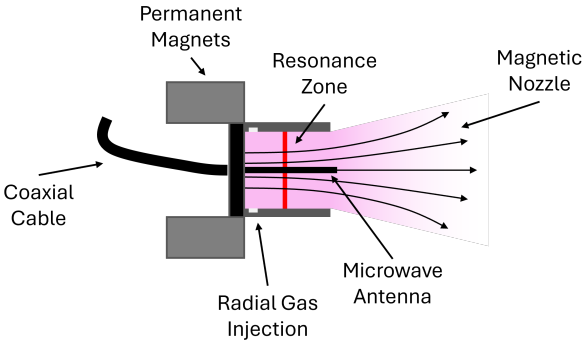

Figure 1. Basic ECR magnetic nozzle thruster schematic.

Operation for an ECR source is as follows: we inject gas into a magnetic environment such that the electrons in this region become magnetized, but the ions do not. Due to the consequences of the Lorentz force, electrons gyrate at a characteristic frequency perpendicular to the magnetic field lines, called the electron cyclotron frequency, $\omega_{c,s} = q_s B/m_s$, where q_s is the charge of the species, B is the magnitude of the magnetic field strength, and m_s is the mass of the species.

As the electrons become magnetized, light at the cyclotron frequency is injected into the gas, causing a resonance effect, enabling energy transfer to the gyrating electrons and production of a plasma. The most efficient energy coupling occurs when light is circularly polarized, oscillating in the same direction as the electron gyration. A common microwave frequency used for ECR sources is 2.45 GHz, which matches a magnitude of applied field strength of 875 Gauss. A well characterized method for microwave injection in ECR thrusters is by use of an antenna that spans axially inside the thruster, which is coupled to an input coaxial line. As energy is transferred to the electrons in the gas, their Larmor radius will increase as $r_l = v_\perp/\omega_{c,s}$, but this species will be able to resonate for the entirety of the resonance region due to the cyclotron period remaining constant, as it has no energy dependence. Because of this sustained energy coupling interaction, electron temperatures grow rapidly.

While free-streaming expansion of hot electrons will produce some thrust on its own, the addition of a magnetic nozzle allows for efficient transfer of electron thermal energy to ion kinetic energy. It is this addition to an ECR device that greatly strengthens its applicability for space propulsion.

Figure 1 shows an example of this field topology in which the field downstream of the exit plane in the ECR thruster can be modeled as divergent. In this configuration, ions are assumed to be sonic near the exit channel, roughly at the ion acoustic speed, $C_s^2 = k_B T_e/m_i$, where k_B is the Boltzmann constant and T_e is electron temperature. Magnetized electrons 'feel' no magnetic force when flowing along field lines since effects of this type only act orthogonally. The consequences of this effect, high mobility, and the free expansion of the species is that electron motion will continue parallel to the field lines, unimpeded. As this happens, electron perpendicular energy will be converted to parallel, and a charge imbalance will begin to grow in the plasma.

As a response to the electrons spatially separating themselves from the ions, the plasma produces an ambipolar electric field, which drives the different species back together to maintain quasi-neutrality. In an ECR source, this electric field accelerates the ions out of the thruster, effectively transferring the microwave energy that was coupled to the electrons to directed ion kinetic energy. At this same time, an electron-dominated diamagnetic current, $\mathbf{j_d}$, results from the diverging field lines producing a gradient in the plasma density and temperature. Through a $\mathbf{j_d} \times \mathbf{B}$ force, the plasma effectively pushes on the ECR thrusters fixed magnets, creating thrust.

B. Efficiency Model for ECR Thrusters

For EP devices, there are several relevant metrics to assess performance. The first one we consider is thrust efficiency or specific impulse, I_{sp}, which which is defined as,

$$I_{sp} = \frac{T}{\dot{m}_p g_0} = \frac{v_{ex}}{g_0}, \tag{1}$$

where T is thrust, $\dot{m}_p$ is propellant mass flow rate, v_e is the exhaust velocity, and g_0 is the gravitational constant at sea level. We also consider total efficiency, which is defined as the ratio of jet power to total input power. We can model this as

$$\eta_T = \frac{T v_{ex}}{2P_{in}} = \frac{T^2}{2\dot{m}_p P_{in}}, \tag{2}$$

where P_{in} is thruster input power[9]. For ECR thrusters, η_t can be decomposed into several efficiency modes,[10]

$$\eta_T = \eta_m \eta_d \eta_e. \tag{3}$$

The first mode, η_m, is the mass utilization efficiency, which is defined as the ratio of ion to neutral mass flow rate, $\dot{m}_i/\dot{m}$. Next, η_d is the divergence efficiency, which measures how collimated the discharge plasma beam is, and can be found by computing $cos^2(\theta_{div})$, where θ_{div} is the divergence angle of the plume. Lastly, η_e represents our energy efficiency and is effectively the ratio of output power to input power from the thruster, P_{out}/P_{in}. Other terms could be considered in this efficiency mode breakdown, like RF coupling and charge utilization efficiency. However, for a 30 W device, it has been shown that 90-99% of RF power is coupled into the gas.[11] It is possible that nitrogen gas can ionize or dissociate into different species, but E×B probe data shows that only singly ionized N_2 existed in our study.

C. Model for Mass Utilization and Role of Electron Temperature

Theoretical investigations into how mass utilization efficiency scales as a function of propellant type have been explored for various EP devices.[6,12] While not specific to ECR thrusters, one relevant model for HETs was derived by Hurley and Jorns that finds

$$\eta_m = 1 - exp\left[-\frac{\langle n_e k_{iz}(T_e)\rangle}{\nu_n}\bar{L}\right], \tag{4}$$

where $\langle n_e k_{iz}(T_e)\rangle$ is the average product of the electron number density and total ionization rate coefficient, $\nu_n = \sqrt{2k_B T_n/\pi m_n}$ as the neutral gas thermal velocity, and $\bar{L}$ is the channel length where ionization is non-negligible and ion acceleration occurs. When compared to nitrogen operation in HETs, the model

is able to match experimental findings for η_m within error and credible intervals. An important aspect of this model is how it predicts the scaling of η_m as a function of electron temperature, T_e. This dependence rests on the relation $k_{iz} \propto \sigma(T_e)$, where $\sigma(T_e)$ is the ionization cross section for a molecule. Straub et al. have experimentally shown that σ increases as a function of electron temperature for electron bombardment ionization up 100 eV.[13] Therefore, this model predicts that mass utilization should increase as a function of increasing ionizing electron temperature, but decrease due to lower neutral mass, which is particularly relevant due to the possibilities of comparatively high electron temperatures inside of ECR thrusters coupled with the lighter molecular mass of nitrogen.

To apply this model to our study, we will assume the following form for electron number density:

$$n_e = \frac{P}{C_s A T_e}. \tag{5}$$

Where P_{in} is the power into the thruster, $C_s^2 = k_B T_e / M_i$ is the ion acoustic speed, A is the area of the thruster, and T_e is the electron temperature. We make use of equation 8 and downstream probe measurements to compute source region electron temperatures. Lastly, we add a linear scaling coefficient, α, for fitting purposes to take into account maximum mass utilization efficiencies < 1 for our ECR device. This gives the final form of the model, therefore as,

$$\eta_m = \alpha \left(1 - exp\left[-\frac{\langle n_e k_{iz}(T_e)\rangle}{\nu_n}\bar{L}\right]\right). \tag{6}$$

D. Evidence for high electron temperature in these devices and implications for nitrogen performance

Near-field plume electron temperatures in a 30 W ECR thruster operating on xenon have been measured near 30 eV, 75 mm downstream from the thruster exit plane.[4] Additionally, several studies have found downstream ion velocities in excess of 17 km/s.[14,15] While not experimentally characterized, this suggests the existence of extremely high electron temperatures in the source region. To crudely estimate this, we can consider an energy balance, with no losses, where the superposition of ion and electron energy is conserved throughout the plume and ions are moving at their acoustic speed in the source region. We can model this energy balance for xenon operation,

$$\frac{5}{2}k_B T_{e0} + \frac{1}{2}m_i C_s^2 = \frac{5}{2}k_B T_{e1} + \frac{1}{2}m_i v_i^2, \tag{7}$$

where $C_s^2 = k_B T_{e0}/m_i$. We can solve for upstream electron temperature as

$$T_{e0} = \frac{5}{6}T_{e1} + \frac{m_i}{6k_B}v_i^2. \tag{8}$$

Plugging in experimentally determined values of $T_{e1} = 30$ eV and $v_i = 15$ km/s, taken 75 mm downstream,[4] we get $T_{e0} \approx 75$ eV. More sophisticated models that leverage both a hybrid particle-in-cell/fluid model and a frequency-domain full-wave finite element model have found that, for 50W operation, these temperatures are closer to 43 eV.[16]. However, electron temperatures near 40 eV does not explain excessive downstream ion velocities. As a comparison, electron temperatures inside HETs operating at 100 W have been shown to peak near 20 eV.[5] One of the key assumptions for the model described by equation 6 is that the average electron temperature in the $\bar{L}$ region scales as $0.1v_d$, where v_d is the discharge voltage of the HET. For the experimental data presented by Hurley and Jorns, nitrogen operation was characterized with a 9-kW class HET with $v_d = 300$ V, indicating $\langle T_e \rangle = 30$ eV. This study found mass utilization efficiencies between 60-90% for operation on nitrogen.[12] Combined with findings that ECR source region electron temperatures possibly could exceed those found in HET by greater than a factor of 2 in similar input power classes,[5] and that mass utilization efficiencies of HET in the 9-kW class, with average electron temperatures near 30 eV, are exceeding 60% , ECR thrusters could be well suited to ionize nitrogen propellant efficiently, even in the $<$ 100 W class.

III. Experimental Setup

In this section we outline the experimental setup as it relates to the facility, thruster, thrust stand, power system, flow system, and far-field probing suite leveraged for this study.

A. Facility, Thruster, and Thrust Stand

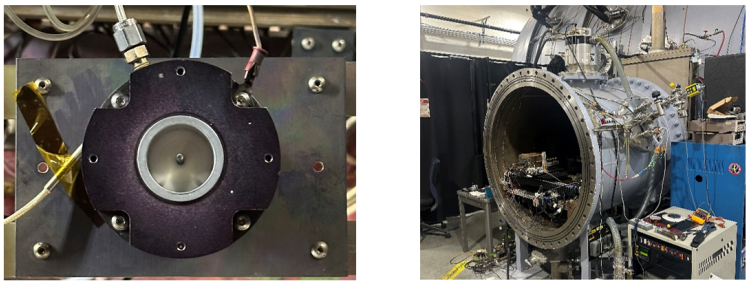

a. b.

Figure 2. a. ECR V2, b. Junior test facility.

To complete our efficiency mode characterization of an ECR magnetic nozzle thruster operating on nitrogen, we performed a far-field probe sweep of the thruster discharge plume. The test article was the ECR V2, seen in figure 2a, an in-house developed 27 mm diameter ECR magnetic nozzle thruster that nominally operates on xenon at 30 W and 1 sccm.[17] The ECR V2 thruster makes use of permanent magnets to form the magnetic nozzle, with a field strength in the resonance region of 875 Gauss. The thruster channel material and backplate are made of boron nitride, and the antenna is graphite.

As can be seen in figure 2b the test facility was the Junior test facility (JTF), which is a 1-meter diameter by 2-meter long cylindrical vacuum chamber housed at the University of Michigan Plasmadynamics and Electric Propulsion Laboratory (PEPL). The JTF can achieve base pressures on the order of 1 μTorr with operating pressures of 5 μTorr for xenon at 1 SCCM and 35 μTorr at 8 SCCM nitrogen operation.

The thrust stand used for these tests was developed and designed by Wachs and Jorns using a hanging pendulum architecture. This design is able to measure thruster from ECR devices with a resolution of 25 μN.[18]

B. Power system

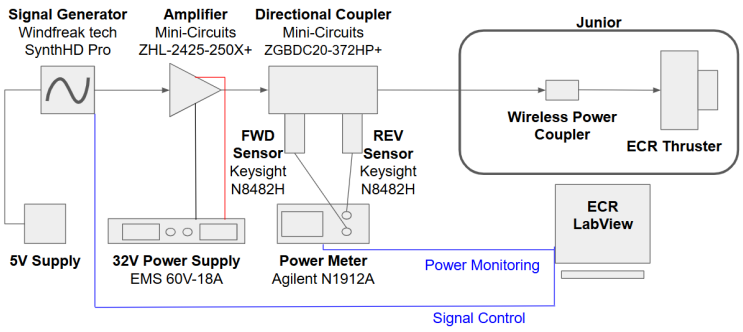

Figure 3. ECR power system diagram.[17]

The ECR thruster power system is outlined in figure 3. The system starts with a dual-output microwave source that generates the initial signal. This is then amplified, and the signal goes through a directional coupler that is connected to a set of two power meters to gauge both forward power and reverse/reflected power from the thruster. Lastly, the microwave power goes through a wireless power coupler that feeds the microwave signal directly to the ECR antenna.[17]

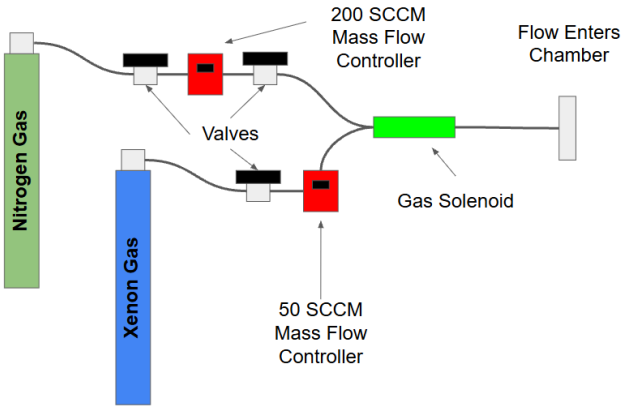

Figure 4. Dual nitrogen and xenon flow system that allowed for consistent thruster lighting at vacuum.

C. Flow System

Previous works operating the ECR V2 thruster on xenon and krypton have shown the thruster lights reliably at vacuum on these propellants.[15] Due to limitations of our setup, lighting the thruster on nitrogen consistently posed a larger challenge than expected. To guarantee lighting at vacuum conditions, we set up a dual flow system in which we could light the thruster on xenon and then slowly transition the gas input to nitrogen, which proved to reliably light a plasma discharge. A diagram of this system can be seen in figure 4.

IV. Diagnostics for characterizing efficiency modes

In this section, we discuss experimental details of each far-field probe leveraged in this study, followed by a discussion of how these measurements are used to compute all relevant efficiency modes for the ECR thruster.

A. ExB Probing

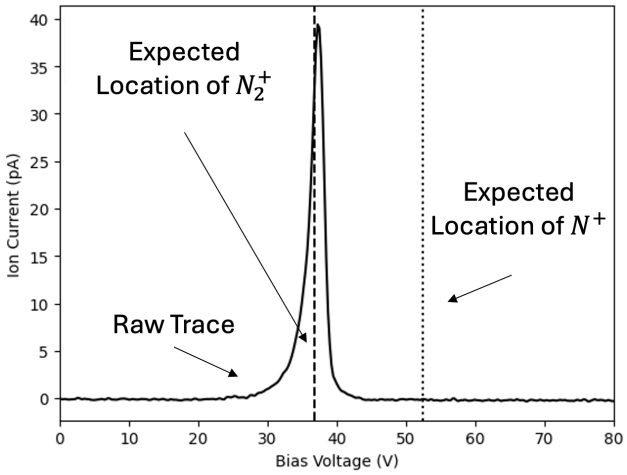

Figure 5. ExB probe trace at 20 W with a single peak, indicating only one ionic species was present in the discharge plume.

Molecular propellants have the possibility of both ionizing and dissociating into several constituent ionic species. If there is more than one population of ions with varying mass or charge, the efficiency mode

calculations become more complex. To examine which ions were being produced, we employed an ExB probe which uses a fixed magnetic field of 1600 G and sweeps over a range of bias voltages from 0 to 100 V between two plates with a distance, d, of 0.381 in between them. As the bias voltage increases, only ions with velocities $v_i = E/B = V_b/Bd$ are able to pass through and register as current. We can compute charge to mass ratios of the ionic species by considering the bias voltages where we see peaks in the current. To do this, we consider a balance of kinetic energy and electric energy.

$$\frac{1}{2}m_i v_i^2 = q_i \bar{V}_i, \tag{9}$$

where $q_i\bar{V}_i$ is average ion energy as measured from an RPA. Using the conversion between ion velocity and bias voltage we can then measure the charge to mass as

$$\frac{q_i}{m_i} = \frac{1}{2}\frac{V_b}{\bar{V}_i B^2 d^2}. \tag{10}$$

The most likely ions we would expect are N_2^+ or N^+, with effective first ionization energies of 15.58 eV and 21.913 eV (dissociation + ionization), respectively.[19–21] An example trace is shown in figure 5, which reflects the results across the input powers investigated, revealing that only N_2^+ ions were being produced. For this reason, the efficiency modes discussed previously only consider contributions from one ion.

B. Langmuir Probing

For the exploration of the ECR far-field plume, we used a cylindrical tungsten Langmuir probe with a length of 10 mm and a diameter of 0.381 mm. The primary motivation for using this probe was to determine plasma potential, V_p, which is necessary to correct RPA measurements. To do so, the probe was swept with bias voltages ranging from -50 to 150 V to collect current from the plasma.

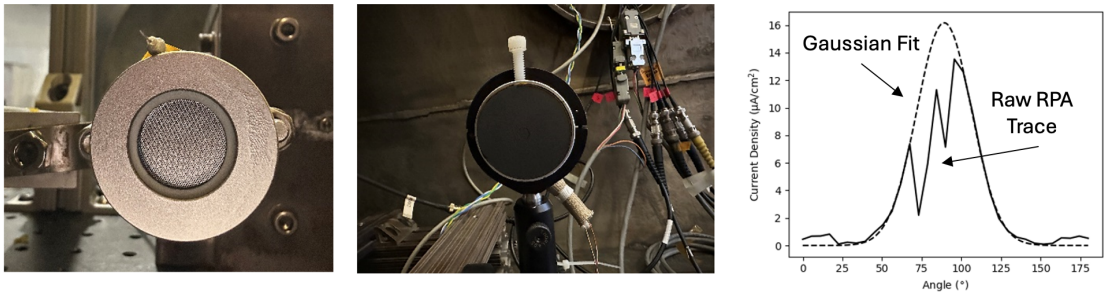

Figure 6. a. RPA with Langmuir probe affixed on the top b. Radial Faraday probe c. Raw Faraday probe trave with Gaussian fit.

After the I-V traces were corrected for ion current effect, we located the knee of the trace by examining the first and second derivatives of the smoothed traces, giving us the plasma potential.[22] Uncertainty in this measurement was found by taking several traces at each operation condition.

C. Retarding Potential Analyzer

As part of the efficiency breakdown for ECR nitrogen operation, we used a retarding potential analyzer (RPA) to determine ion potential downstream of the plasma discharge. This device can measure the ion energy distribution function by making use of several biased grids and sweeping bias voltage from 0 to 120 V to collect current data. To process these traces correctly, we subtract the plasma potential for that operating condition from the raw trace, which is then smoothed and differentiated with respect to the bias potential. A Gaussian fit is then applied to the negative of the smoothed, differentiated trace, and the mean of this fit is the most probable ion energy, $\bar{V}_i$, in units of J/C.[23] Since I_{sp} scales linearly with exhaust velocity, we want to determine how fast the ions in the plume are moving. To determine ion velocities, we can convert from ion energy to kinetic energy as,

$$q_i \bar{V}_i = \frac{1}{2} m_i \bar{v}_i^2. \tag{11}$$

Where q_i is the ion charge, $\bar{V}_i$ is the mean ion electric potential, m_i is the ion mass, and $\bar{v}_i$ is the average ion velocity. We can rearrange equation 9 giving our average ion velocity,

$$\bar{v}_i = \sqrt{\frac{2 q_i \bar{V}_i}{m_i}} \tag{12}$$

D. Faraday Probe

The last necessary instrument for our characterization is a Faraday probe, which we leveraged to compute ion beam current densities, $j(\theta)$, in the thruster plume. Faraday probes are designed such that there is an outer guard ring and an inner collector separated by a distance on the scale of a plasma Debye length. For our study, the guard ring was biased to 100 V and placed at a fixed radial distance from the ECR thruster discharge plasma. This probe was swept radially across the thruster face 180 degrees. To compute total and axial ion currents from these traces, we integrate with respect to the swept angle between the thruster face and probe arm, θ,

$$I_{beam} = 2\pi R^2 \int_0^{\pi/2} j(\theta) cos(\theta) d\theta \tag{13}$$

and

$$I_{ax} = 2\pi R^2 \int_0^{\pi/2} j(\theta) sin(\theta) cos(\theta) d\theta \tag{14}$$

where R is the radial distance from the thruster face to the probe [24].

Other studies using radial Faraday probing on ECR thruster have biased the guard ring in excess of 300 V to fully repel electrons. [25] We found in this study that there was a trade-off between detrimental thruster arcing and this electron repelling. Because of this, a Gaussian was fit to our Faraday traces to serve as a proxy for the ion current density (see figure 6c). This adds a source of uncertainty, which is reflected in our results.

E. Efficiency Modes

Given the average ion energies found with the RPA and Langmuir probe and both total and axial components of the downstream ion beam current measured from the Faraday probe, we can compute all relevant efficiency modes as outlined previously in section II. Divergence efficiency, η_d, is defined as $cos^2\theta_{div}$, where θ_{div} is the divergence angle of the plume. We can compute $\theta_{div} = arccos(I_{ax}/I_{beam})$, which means we can estimate our divergence efficiency as,

$$\eta_d = \left(\frac{I_{ax}}{I_{beam}} \right)^2. \tag{15}$$

To determine our energy efficiency, we can re-write the power output of the thruster as a function of I_{beam}, $P_{out} = I_{beam} \bar{V}_i$. This results in the energy efficiency given as

$$\eta_e = \frac{I_{beam} \bar{V}_I}{P_{in}}. \tag{16}$$

Lastly, to compute mass utilization efficiency, η_m, we can re-write ion mass flow rate as $\dot{m}_i = I_{beam} m_i / q_i$, resulting in the final expression for η_m,

$$\eta_m = \frac{I_{beam} m_i}{q_i \dot{m}_p}. \tag{17}$$

V. Results

In this section, we present the results from the nitrogen characterization of the ECR V2 thruster at various powers with a fixed flow rate of 8 SCCM. When appropriate, this data is plotted against xenon operation results at 1SCCM in the same thruster and facility from Eckhaus et al. 2025.[15] This section concludes with a discussion of the results.

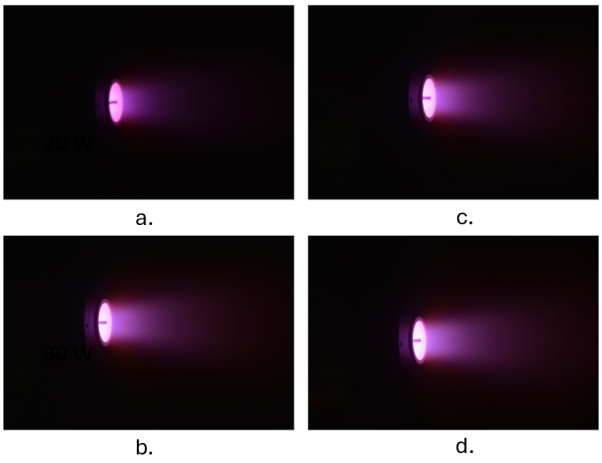

Figure 7. ECR V2 thruster operating on nitrogen at a 20 W, b 30 W, c 40 W, and d 50 W.

A. Global Performance

Figures 8b and c show the results for specific impulse, I_{sp}, and overall efficiency, η_t, as a function of power at fixed flow rate. As can be seen, the ECR operation on nitrogen produces < 400 s specific impulses and general efficiencies peaking at 2% when estimated by thrust measurements. As a comparison, Eckhaus et al. have achieved nearly 1000 s of I_{sp} and nearly 10% total efficiency while operating on xenon and otherwise the same thruster and input powers. The comparatively low specific impulse is surprising since the mass of N_2 ions is small compared to that of xenon, implying that the exhaust speed should increase for ECR operation on this gas for a given temperature.

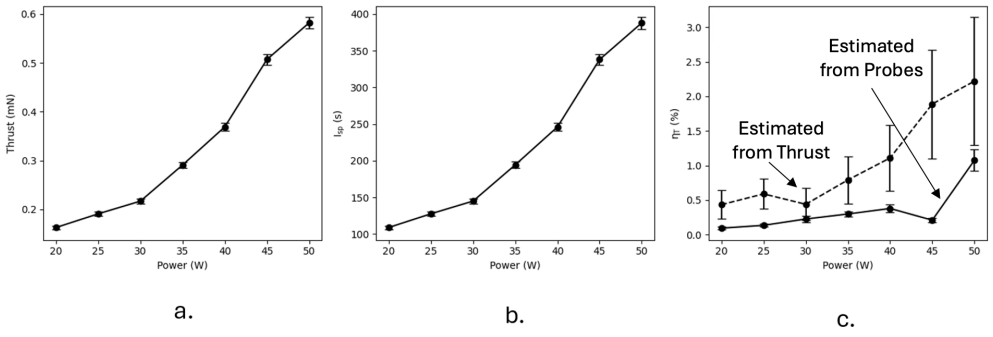

Figure 8. As a function of power a. Thrust, b. I_{sp}, and c. η_t estimated from thrust and prone measurements.

In practice, this lower specific impulse may be explained by lower mass utilization efficiency. We return to this point in sections V and VI.

Figure 9 shows the estimated downstream average ion velocities, which exceed the xenon average, despite comparatively seeing more than an 50% drop in specific impulse. Therefore, global performance metrics are not enough to reveal why the thruster is operating below 2% efficiencies. To fully diagnose the source of this inefficiency, we must now consider the decomposed efficiency modes detailed in sections II and IV.

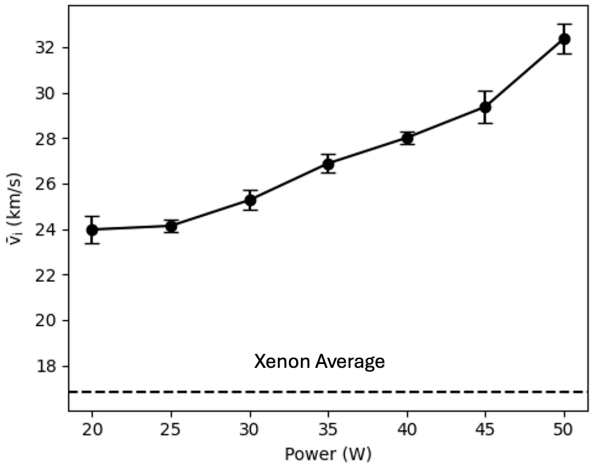

Figure 9. Downstream ion average velocities computed from the RPA probe as a function of power.

B. Efficiency Modes

The first mode to consider is η_d in figure 10a, which reveals that the nitrogen discharge from the thruster is more collimated than xenon, and is therefore not a significant source of efficiency loss. Figure 10b reveals that the energy efficiency, η_e, is quite low, which plays a role in the overall lower total efficiency. However, $\eta_e \propto I_{beam}$, which means our energy efficiency is coupled to total output current, or simply the number of ions that the thruster is producing. This suggests that the root of ECR performance issues lies with mass utilization.

Figure 10c shows that η_m is indeed the lowest efficiency mode across all the powers investigated. Like the energy mode, $\eta_m \propto I_{beam}$, but is not proportional to the amount of energy being deposited to the ions, indicating this is the largest loss of efficiency for ECR nitrogen operation. Moreover, these results suggest that so few ions are being produced that any potential boost in global performance from comparatively quicker ions is greatly offset.

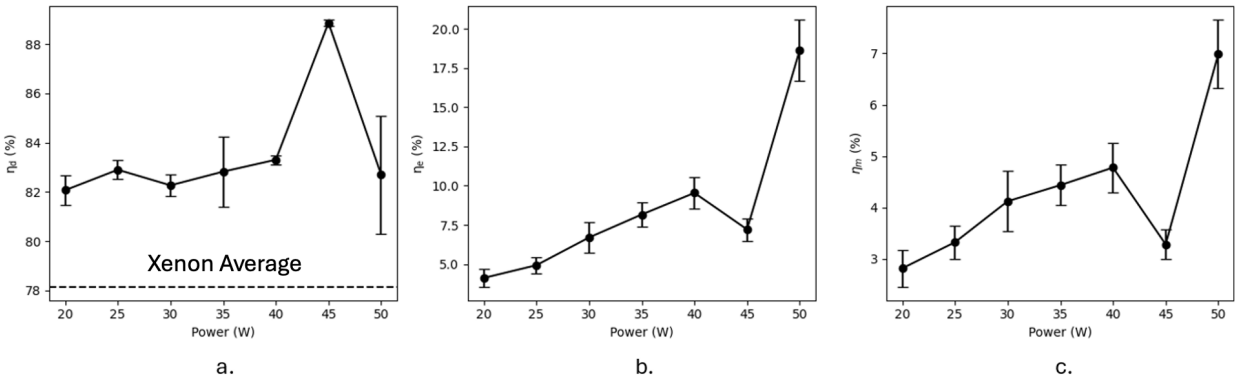

Figure 10. a. Beam divergence and b. Energy, and c. Mass utilization efficiency as functions of power.

VI. Discussion

In this section, we discuss our results in the context of equation 6, error in relation to comparatively higher operational pressures for nitrogen ECR operation, and propose how to increase thruster performance on this propellant.

A. Evaluation of Mass Utilization model

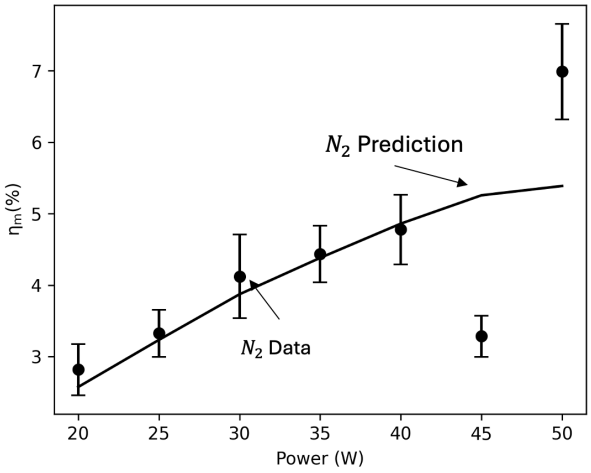

Figure 11. Equation 6 regressed to the nitrogen data.

The results of our study indicate that ion production, and therefore mass utilization, are likely the cause of poor thruster performance when operating on nitrogen gas. This result falls in line with work by Sheppard and Little that had similar findings for ECR operation with water as a propellant.[6] This potentially leaves open questions about ECR thruster electron temperatures exceeding the predicted 70 eV in the source region, since this should have led to higher mass utilization. However, it is possible that low densities might be counteracting any boost in efficiency we might see from these hot electrons. In section II, equation 6 was proposed as a possible model for scaling of mass utilization. In the original derivation by Hurely and Jorns,[12], it is assumed that $\bar{L}$, the length of the channel where ionization is non-zero, is a free parameter to be learned from experimental data. Regressing equation 6 against xenon mass utilization data collected by Eckhaus and Jorns suggests that $\alpha \approx 0.57$. By assuming this is our 'true' maximum η_m, we can regress equation 6 against our nitrogen results, suggesting that $\bar{L} = 0.45$ mm. This regression can be seen in figure 11. To further contextualize this result, we can also examine the effective neutral residence time, $\bar{L}/v_n$, which is 2 μs. Both of these values motivate why mass utilization efficiency is so low for nitrogen operation, as the length or time that an N_2 molecule could reasonably ionize is extremely small. This suggests that a focus for increasing ECR thruster performance on alternative propellants should possibly aim to maximize $\bar{L}$ when considering thruster configurations and operating conditions. Immediately, the results in figure 11 suggest that mass utilization will continue to increase beyond the chosen operating powers for this study, suggesting future work should aim to explore higher delivered power conditions to optimize thruster performance on nitrogen.

B. High Operational Pressures

Another effect from the comparatively high nitrogen flow rates we used is the known relationship between operating pressure and performance of ECR thrusters.[26] Because ECR operation on nitrogen required 8 times as much volumetric flow as xenon, we found correspondingly that operational pressure for nitrogen was roughly 8 times as high. Wachs and Jorns 2018 revealed that ion energy decreases as a function of increasing operational pressure for ECR thrusters, revealing an approximate 40 eV drop in ion energy 10 cm downstream between operational pressures of 0.98 and 26 μTorr (a similar range between nitrogen and xenon operation).[26] It is currently unclear how this effect would scale to nitrogen as a propellant, but since $\eta_e \propto \bar{V}_i$, we can compute what a 40 eV increase in ion energy corresponds to, which is roughly a 3-5% increase in energy efficiency, meaning this effect is likely a small source of error in our computation of total efficiency.

C. ECR Thruster Configuration Change

The results from our study and equation 6 suggest that we are not ionizing efficiently, and the reason for this might have to do with the small residence time, or effective ionization length, for nitrogen in our thruster. To combat this, a possible solution could be to extend the channel length. The downside of this adjustment would be increased magnetic flux through the walls, which could increase wall losses from magnetized electrons. However, as seen in figure 10a, the nitrogen discharge beam is more collimated than xenon, which could mean that much of the ionization is occurring near the antenna and center of the thruster channel. Evidence of this can be seen in figure 6c with the raw RPA trace, where as the probe gets closer to being parallel with the thruster face, highly energetic electrons are able to overcome the 100 V bias on the guard. This indicates that much of the highly energetic electrons are exiting the thruster mainly on the central field lines. This could indicate that increasing the channel length might be successfully done while minimally increasing wall losses. An alternative approach to extending the channel length is to design a cone that roughly follows the diverging field lines.[25] This would increase neutral confinement, while also minimizing losses from increasing the channel length only in the axial direction. Another change to consider would be to the propellant injection scheme for the thruster. It has been found that adding partial downstream propellant injection for helicon devices can improve overall thruster performance, and as it relates to ECR nitrogen operation, ion production.[27]

VII. Conclusions

The ECR V2 thruster performed at peak specific impulses and total efficiencies of nearly 400 s and 2% for nitrogen operation, which is a significant reduction from xenon in the same thruster and input powers. To figure out why, we leveraged a far-field probe suite to assess the primary cause of these performance issues, which revealed that mass utilization for ECR nitrogen operation was more than 40% less than that of xenon operation,[15] to the effect that thrust, Isp, and η_t suffered, despite higher downstream ion velocities. We asserted in section II that higher electron temperatures produced in the ECR source region could offset difficulties with ionizing nitrogen; however, it is likely that a combination of electron density, temperature, and residence time are too low to ionize nitrogen effectively. To further this point, we regressed a 1D HET model for mass utilization efficiency and found that this residence time is on the order of 2 μs. Trends in the data suggest future work should test ECR nitrogen operation with a possibly longer channel length or a cone configuration to confine neutrals better, while possibly considering more exotic propellant injection schemes to enable better ionization, while exploring higher delivered power conditions.

VIII. Acknowledgments

This work was funded by the Air Force Office of Scientific Research Grant #FA9550-25-1-0025 under the Space Power and Propulsion Portfolio

References

[1] T. Andreussi *et al.*, "A review of air-breathing electric propulsion: from mission studies to technology verification," *Journal of Electric Propulsion*, vol. 1, p. 31, 2022.

[2] N. H. Crisp *et al.*, "The benefits of very low earth orbit for earth observation missions," *Progress in Aerospace Sciences*, 2020.

[3] D. Di Cara, J. Gonzalez del Almo *et al.*, "Ram electric propulsion for low earth orbit operation: an esa study," *the 30th International Electric Propulsion Conference*, 2007.

[4] S. Correyero *et al.*, "Plasma beam characterization along the magnetic nozzle of an ecr thruster," *Plasma Sources Sci. Technol. 28*, 2019.

[5] A. Smirnov, "Plasma measurements in a 100 w cylindrical hall thruster," *Journal of Applied Physics*, 2003.

[6] A. J. Sheppard and J. M. Little, "Performance analysis of an electron cyclotron resonance thruster with various propellants," *Journal of Propulsion and Power*, vol. 38, no. 6, pp. 998–1007, 2022.

[7] R. Maoloney *et al.*, "Experinetal validation and performance measurements of an ecr thruster operating on multiple propellants." *36th International Electric Propulsion Conference*, 2019.

[8] P. Svarnas, *Electron cyclotron resonance (ECR) plasmas: A topical review through representative results obtained over the last 60 years.* J.Appl. Phys, 2017.

[9] D. M. Goebel and I. Katz, *Fundamentals of Electric Proplusion: Ion and Hall Thrusters 2nd Edition.* JPL Science and Technology Series, 2008.

[10] J. Jarrige *et al.*, "Performance comparison of an ecr plasma thruster using argon and xenon as propellant gas," *33rd International Electric Propulsion Conference*, 2013.

[11] V. Desangles *et al.*, "Ecra thruster latest development at onera: Focus on thrust vectoring activities," *Aerospace Europe Conference*, 2023.

[12] W. J. Hurley and B. A. Jorns, "Mass utilization scaling with propellant type on a magnetically shielded hall thruste," *Plasma Sources Sci. Technol. 34 055010*, 2025.

[13] H. C. Straub *et al.*, "Absolute partial cross sections for electron-impact ionization of h2, n2, and o2 from threshold to 1000ev," *Physical Review A*, 1995.

[14] V. Désangles, S. Peterschmitt, D. Packan, and J. Jarrige, "Ecra thruster advances, 30w and 200w prototypes latest performances," in *37th International Electric Propulsion Conference.* Electric Rocket Propulsion Society, 2022.

[15] A. Eckhaus and B. Jorns, "Experimental investigation of wall material effects in electron cyclotron resonance thrusters," *the 39th International Electric Propulsion Conference*, 2025.

[16] A. Sanches-Villar *et al.*, "Coupled plasma transport and electromagnetic wave simulation of an ecr thruster," *Plasma Sources Sci. Technol 30*, 2021.

[17] B. N. Wachs, "Optimization and characterization of facility effects for a low power electron cyclotron resonance magnetic nozzle thruster," Ph.D. dissertation, University of Michigan, 2022.

[18] B. Wachs and B. Jorns, "Sub-millinewton thrust stand and wireless power coupler for microwave-powered small satellite thrusters," *Review of Scientific Instruments, 93(8), 083507*, 2022.

[19] NIST. Nitrogen. [Online]. Available: https://webbook.nist.gov/cgi/cbook.cgi?ID=C7727379&Mask=20

[20] NIH. Ionization energy in the periodic table of elements. [Online]. Available: https://pubchem.ncbi.nlm.nih.gov/ptable/ionization-energy/

[21] A. G. Gaydon, "Dissociation energy of nitrogen," *Nature*, 1944.

[22] R. Lobbia *et al.*, "Reccomended practice for use of langmuir probes in electric propulsion testing," *Journal of Propulsion and Power Vol. 33, Number 3*, 2017.

[23] S. T. Lai *et al.*, "Retarding potential analyzer: Principles, designs, and space applications," *AIP Advances 10*, 2017.

[24] D. L. Brown *et al.*, "Recommended practice for use of faraday probes in electric propulsion testing," *Journal of Propulsion and Power Vol. 33, No, 3*, 2017.

[25] O. Hitchens, "Performance increase of electron cyclotron resonance magnetic nozzle thruster via magnetically thickened resonance region," Ph.D. dissertation, University of Surrey, 2025.

[26] B. Wachs and B. Jorns, "Background pressure effects on ion dynamics in a low-power magnetic nozzle thruster," *Plasma Sources Sci. Technol.*, 2020.

[27] K. Takahashi *et al.*, "Modifications of plasma density profile and thrust by neutral injection in a helicon plasma thruster," *Applied Physics Letters 109*, 2016.